

# In Vitro and In Ovo Expression of Chicken Gamma Interferon by a Defective RNA of Avian Coronavirus Infectious Bronchitis Virus

Karen Hackney, Dave Cavanagh, Pete Kaiser, and Paul Britton\*

*Institute for Animal Health, Compton Laboratory, Compton, Newbury, Berkshire RG20 7NN, United Kingdom*

Received 25 November 2002/Accepted 28 February 2003

**Coronavirus defective RNAs (D-RNAs) have been used for site-directed mutagenesis of coronavirus genomes and for expression of heterologous genes. D-RNA CD-61 derived from the avian coronavirus infectious bronchitis virus (IBV) was used as an RNA vector for the expression of chicken gamma interferon (chIFN- $\gamma$ ). D-RNAs expressing chIFN- $\gamma$  were shown to be capable of rescue, replication, and packaging into virions in a helper virus-dependent system following electroporation of in vitro-derived T7 RNA transcripts into IBV-infected cells. Secreted chIFN- $\gamma$ , under the control of an IBV transcription-associated sequence derived from gene 5 of the Beaudette strain, was expressed from two different positions within CD-61 and shown to be biologically active. In addition, following infection of 10-day-old chicken embryos with IBV containing D-RNAs expressing chIFN- $\gamma$ , the allantoic fluid was shown to contain biologically active chIFN- $\gamma$ , demonstrating that IBV D-RNAs can express heterologous genes in vivo.**

Infectious bronchitis virus (IBV) is a highly infectious and economically important pathogen of chickens that causes respiratory disease, diminished growth rate, and substantial decline in egg production. Although infectious bronchitis is considered primarily a disease of the respiratory system, strains of IBV have wide and variable tropisms and the clinical manifestations of the disease can be diverse (9). Genetically very similar viruses cause disease in turkeys (6) and pheasants (7). IBV is a group 3 member of the genus *Coronavirus* of the family *Coronaviridae* in the order *Nidovirales* (12), being an enveloped RNA virus with an unsegmented, 5'-end-capped, 3'-end-polyadenylated, single-stranded, positive-sense RNA genome of 27,608 nucleotides (nt) (4). Coronaviruses produce a 3'-coterminal nested set of subgenomic mRNAs (sg mRNAs) that are polycistronic. These are produced by a discontinuous transcription process during synthesis of the negative strand and contain identical 5' ends due to the addition of a leader sequence derived from the 5' end of the genomic RNA (gRNA) (35, 36). Preceding the body sequence of each sg mRNA is a consensus sequence, the transcription-associated sequence (TAS) (15), involved in the acquisition of the leader sequence. All coronavirus envelopes contain at least three membrane proteins, the spike glycoprotein, a small membrane protein, and an integral membrane protein. In addition, the coronavirus virion also contains a nucleocapsid protein that interacts with the gRNA.

Coronavirus defective RNAs (D-RNAs), which lack large parts of the genome, are produced following virus passage at a high multiplicity of infection. While all D-RNAs contain *cis*-acting sequences necessary for replication, only a subset of D-RNAs contain sequences necessary for packaging into virions in the presence of a helper virus. Coronavirus D-RNAs have been used for site-directed mutagenesis of the virus ge-

nome (25) and for expression of heterologous genes (1, 2, 13, 17, 20, 22, 39, 42, 43).

Cytokines are regulatory proteins that act as a communication network between cells throughout immunological development. Avian homologues of several mammalian cytokines have been isolated, including chicken gamma interferon (chIFN- $\gamma$ ) (10). Mammalian IFN- $\gamma$  is a pleiotropic cytokine initially produced by natural killer cells, during immune induction, and then by committed T helper 1 (Th1) cells as a regulator and effector molecule for driving inflammatory responses (for a review, see reference 8). IFN- $\gamma$  has a major role in activating antiviral immune responses through augmentation of major histocompatibility complex expression on antigen-presenting cells for interaction with T cells, stimulation of antibody (Ab) formation, promotion of Ab isotype class switching, and development of cytotoxic T cells. Several studies have been undertaken to investigate the in vivo potential of IFN- $\gamma$  as a vaccine adjuvant. Coadministration of bovine IFN- $\gamma$  with vesicular stomatitis virus G glycoprotein to cattle resulted in an increased formation of protective Ab against vesicular stomatitis virus (41). In a mouse model, fusion of IFN- $\gamma$  to human immunodeficiency virus gp120 resulted in enhanced primary Ab responses against gp120, enhanced antigen-specific T-cell proliferation, and IFN- $\gamma$  production (26). The use of recombinant feline IFN- $\gamma$  as a vaccine adjuvant increased Ab responses against rabies virus and calicivirus antigens (37).

The role of recombinant chIFN- $\gamma$  as an adjuvant and therapeutic agent has been investigated. Coadministration of chIFN- $\gamma$  with sheep red blood cells (SRBCs) resulted in an increased secondary Ab response with amounts of SRBCs 10-fold smaller than the dose of SRBCs given alone (23, 24). Administration of recombinant chIFN- $\gamma$  prior to challenge with avian coccidia resulted in decreased intracellular sporozoite development and oocyst production, with an enhanced level of body weight gain (21). chIFN- $\gamma$  had an adjuvant effect, reducing parasite replication, when used in a DNA vaccine regimen against *Eimeria acervulina* (27). Coexpression of New-

\* Corresponding author. Mailing address: Division of Molecular Biology, Institute for Animal Health, Compton Laboratory, Compton, Newbury, Berkshire RG20 7NN, United Kingdom. Phone: 44 1635 578411. Fax: 44 1635 577263. E-mail: paul.britton@bbsrc.ac.uk.

TABLE 1. Oligonucleotides used for generation of TAS-chIFN- $\gamma$  cassette and hybridization probes

Oligonucleotide	Sequence <sup>a</sup>	Position <sup>b</sup>	Polarity
IBV5IFN- $\gamma$ START	TCC CCC GGG CAC GTG TTT TAC TTA ACA AAA ACT TAA CAA ATA CGG ACG ATG ACT TGC CAG ACT	NA	+
SmallIFN- $\gamma$ -END	ACC CCC GGG GGT TAG CAA TTG CAT CT	NA	-
BG-67	GGC TGG TTC GAG TGC GAG	Beaudette 265–282	-
BG-2	TCA GGG GTT GTT TGG CAC T	Beaudette 455–473	-
IFN/3	ATG ACT TGC CAG ACT TAC AA	chIFN- $\gamma$ 1–20	+
IFN/7	CAG GTC CAT GAT ATC TTT CAC	chIFN- $\gamma$ 340–360	-

<sup>a</sup> Underlined sequences correspond to the IBV sequence. Nucleotides marked in bold correspond to the IBV canonical TAS, and those in italics correspond to restriction endonuclease sites used for cloning.

<sup>b</sup> The positions of the nucleotides refer to the IBV Beaudette sequence (4) or the chIFN- $\gamma$  sequence (10). NA, not applicable.

castle disease virus antigens with chIFN- $\gamma$  by using fowlpox virus resulted in an earlier Ab response, with the best protective immune response of the recombinant fowlpox virus vaccines (32).

In this study we describe both the *in vitro* and *in ovo* expression of biologically active chIFN- $\gamma$  from an IBV D-RNA. We demonstrate for the first time the expression of a chicken cytokine from an IBV D-RNA and the *in ovo* expression of a biologically active heterologous gene from an IBV D-RNA.

#### MATERIALS AND METHODS

**Cells and viruses.** IBV Beaudette was grown in 11-day-old embryonated domestic fowl eggs, harvested from allantoic fluid 24 h postinfection, and used as helper virus for the rescue of IBV D-RNAs (31). IBV was passaged and titrated on primary chick kidney (CK) cells (30). HD11 cells, an avian leukosis virus (MC29)-transformed cell line (3), were cultured in RPMI 1640 medium (Life Technologies) containing 2.5% fetal calf serum, 2.5% chick serum, 10% tryptose phosphate broth, 20 mM L-glutamine, 0.225% NaHCO<sub>3</sub>, 1 U of penicillin/ml, and 1  $\mu$ g of streptomycin/ml.

**Oligonucleotides.** The oligonucleotides used in this work were obtained from Invitrogen and are listed in Table 1.

**Recombinant DNA techniques.** Standard procedures were used to produce recombinant DNA (33), or methods were according to the manufacturers' instructions.

**Construction of TAS-chIFN- $\gamma$  gene cassette.** A TAS-chIFN- $\gamma$  cassette was produced by PCR for insertion into the IBV D-RNA CD-61 cDNA sequence in pIBV-Vec (13). Oligonucleotides IBV5IFN- $\gamma$ START and *Sma*IIFN- $\gamma$ -END, corresponding to the 5' end and complementary to the 3' end, respectively, of the chIFN- $\gamma$  sequence, were used to generate the TAS-chIFN- $\gamma$  cassette. Oligonucleotide IBV5IFN- $\gamma$ START contained the restriction endonuclease *Sma*I and *Pma*CI sites, the Beaudette-derived gene 5 TAS (39), and the first 15 nt of the chIFN- $\gamma$  sequence. Oligonucleotide *Sma*IIFN- $\gamma$ -END consisted of the last 15 nt (complementary) of the chIFN- $\gamma$  gene, including the termination codon, followed by a *Sma*I site. The chIFN- $\gamma$  sequence was amplified by PCR by using *Taq*/*Pwo* DNA polymerase (Hybaid) from plasmid pGEM-T-IFN- $\gamma$  (19) containing a cDNA derived from chIFN- $\gamma$  mRNA. The TAS-chIFN- $\gamma$  cassette was digested with *Xma*I and ligated into *Xma*I-digested pBluescript II SK(+) (Stratagene), resulting in pBS-IFN- $\gamma$ +ENDS, in which the TAS-chIFN- $\gamma$  sequence was verified by sequence analysis. The TAS-chIFN- $\gamma$  cassette was removed from pBS-IFN- $\gamma$ +ENDS by using *Pma*CI and *Sma*I and inserted into either the *Pma*CI site or the *Sna*BI site in the CD-61 sequence of pIBV-Vec.

**In vitro rescue of chIFN- $\gamma$ -containing D-RNAs by IBV Beaudette.** *In vitro* T7-derived D-RNA transcripts were synthesized from 1  $\mu$ g of plasmid DNA and electroporated into IBV-infected CK cells (passage 0 [P<sub>0</sub>]) (39). Virus V<sub>1</sub> in 1 ml of cell medium was used to infect CK cells, and viruses V<sub>2</sub> to V<sub>6</sub> were serially passaged every 24 h for six passages (P<sub>1</sub> to P<sub>6</sub>).

**In ovo rescue of chIFN- $\gamma$ -containing D-RNAs.** Cell medium (100  $\mu$ l) from P<sub>3</sub> CK cells, corresponding to peak D-RNA levels, was used to infect 10-day-old Rhode Island Red specific-pathogen-free embryos. The infected embryos were incubated at 37°C for 16 h and cooled to 4°C overnight. Allantoic fluid was collected from the infected eggs, centrifuged at 1,500  $\times$  g for 10 min, and stored at -70°C. Allantoic fluid (100  $\mu$ l) containing IBV and any potential D-RNA was used to infect CK cells.

**Identification of IBV-derived RNAs.** Total cytoplasmic RNA was extracted from infected CK cells by using RNeasy (Qiagen) and electrophoresed in denaturing 1% agarose–2.2 M formaldehyde gels. The RNAs were Northern blotted onto Hybond XL nylon membranes (Amersham), and IBV-derived RNAs were detected with probes covalently labeled with psoralen-biotin (BrightStar; Ambion) (13). The probes were hybridized to the RNAs at 42°C for 16 h, detected with streptavidin-alkaline phosphatase conjugate in the presence of an alkaline phosphatase 1,2-dioxetane chemiluminescent substrate (CDPStar and BrightStar Biodetect; Ambion), and exposed to film at room temperature for 2 h. An IBV-specific 309-nt 3'-untranslated region (UTR) probe, corresponding to the last 309 nt of the 3' end of the IBV genome, was used to detect all IBV-derived RNA species, including IBV-derived D-RNAs (13). A 209-nt 5' IBV-specific probe, produced by PCR with oligonucleotides BG-67 and BG-2 (Table 1) corresponding to nt 265 to 474 within the 5' UTR of the Beaudette genome, was used to detect IBV gRNA and D-RNAs. A 360-nt chIFN- $\gamma$ -specific probe, produced by PCR with primers IFN/3 and IFN/7 (Table 1), was used to detect RNAs containing the chIFN- $\gamma$  sequence.

**chIFN- $\gamma$  bioassays and neutralization assays.** The chIFN- $\gamma$  bioassays and neutralization assays were carried out as described by Lawson et al. (19). Essentially, triplicate samples (200  $\mu$ l) of serially diluted CK cell medium or allantoic fluid, either from mock-infected embryos or embryos infected with IBV, were added to 4  $\times$  10<sup>4</sup> HD11 cells in 96-well flat-bottomed plates. Recombinant chIFN- $\gamma$ , prepared as described by Lawson et al. (19), was serially diluted two-fold and used as a positive control. chIFN- $\gamma$  neutralization assays were carried out by using an anti-chIFN- $\gamma$  neutralizing monoclonal Ab (MAb), 1E-12 (18), and an anti-bovine granulocyte-macrophage colony-stimulating factor polyclonal Ab, CC305 (kindly provided by Paul Sopp, Institute for Animal Health, Compton, United Kingdom). Both antibodies were diluted 1:1,000 and incubated with CK cell medium and allantoic fluid samples for 2 h at room temperature before being added to HD11 cells. For controls, all samples were also preincubated with the isotype control Ab CC305 and media alone. All HD11 cells were incubated at 41°C in 5% CO<sub>2</sub> for 48 h for the chIFN- $\gamma$  bioassays.

Nitric oxide (NO) produced from HD11 cells, resulting from induction with chIFN- $\gamma$ , was measured in HD11 cell medium (100  $\mu$ l) as nitrite (NO<sub>2</sub><sup>-</sup>) by using a modification of the Griess assay described by Lawson et al. (19) and a Spectra Max 250 enzyme-linked immunosorbent assay reader (Molecular Devices, Wokingham, United Kingdom). The amount of NO present in the HD11 cell media was expressed as the concentration of NO<sub>2</sub><sup>-</sup> (millimolar) for the chIFN- $\gamma$  bioassays or as the optical density at 543 nm for the neutralizing assays.

#### RESULTS

**D-RNAs containing TAS-chIFN- $\gamma$ .** Expression of heterologous genes from coronavirus D-RNAs requires the genes to be under the control of a TAS for synthesis of an sg mRNA. The chIFN- $\gamma$  sequence was placed under the control of the IBV Beaudette gene 5 TAS (39) by using PCR and a chIFN- $\gamma$  mRNA-derived cDNA (19), generating a TAS-chIFN- $\gamma$  cassette for IBV-controlled expression. The gene 5 TAS was originally chosen for expression of heterologous genes because it has the shortest sequence between the 3' end of the TAS and the AUG of open reading frame (ORF) 5a and also because the Beaudette sg mRNA 5 is one of the most abundantly

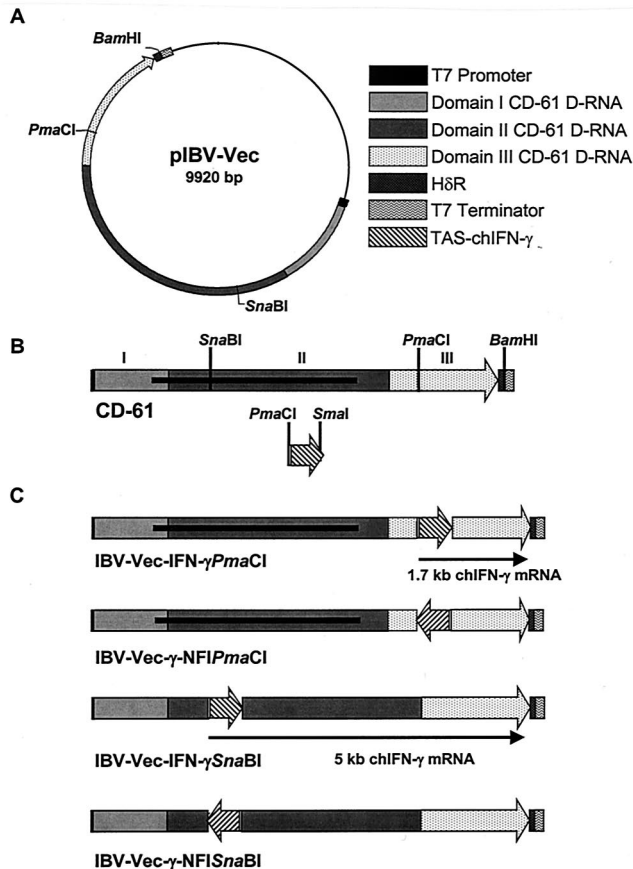


FIG. 1. Schematic diagrams of the IBV D-RNAs containing the TAS-chIFN- $\gamma$  sequence. (A) pIBV-Vec showing the *PmaCI* and *SnaBI* sites within CD-61 for insertion of heterologous genes. H8R, hepatitis delta virus antigenomic ribozyme. (B) IBV D-RNA CD-61, showing the positions of the restriction sites. The *BamHI* site was used for determining the orientation of inserts. The TAS-chIFN- $\gamma$  gene cassette was used for insertion into CD-61. The 998-amino-acid CD-61-specific ORF (30, 31) is indicated as a thick black line. (C) The D-RNAs resulting from insertion of the TAS-chIFN- $\gamma$  cassette into the two restriction endonuclease sites, in both orientations, within CD-61. The T7 promoter, H8R, and T7 termination sequences of pIBV-Vec (13) and the TAS-chIFN- $\gamma$  sequences are as indicated in panel A. The chIFN- $\gamma$  mRNAs of 1.7 and 5.0 kb derived from D-RNAs IBV-Vec-IFN- $\gamma$ -*PmaCI* and IBV-Vec-IFN- $\gamma$ -*SnaBI*, respectively, are indicated as black arrows.

expressed sg mRNAs (39). The TAS-chIFN- $\gamma$  cassette was initially inserted into pBluescript II SK(+) under the control of the T7 promoter. A protein with a size corresponding to that of chIFN- $\gamma$  was produced in vitro by using the TNT T7 coupled wheat germ extract system (Promega; data not shown), indicating that a product of the expected size could be produced from the TAS-chIFN- $\gamma$  cassette.

Two restriction endonuclease sites, *PmaCI* and *SnaBI*, within the IBV D-RNA CD-61 have been used for the expression of heterologous genes (13, 39). The *PmaCI* site is within domain III of CD-61 and not within the D-RNA-specific ORF (31), whereas the *SnaBI* site, within domain II of CD-61, interrupts the D-RNA-specific ORF (Fig. 1B). The TAS-chIFN- $\gamma$  cassette excised from pBS-IFN- $\gamma$ +ENDS was inserted into the *PmaCI* site or the *SnaBI* site of the CD-61

sequence in pIBV-Vec. Four plasmids, pIBV-Vec-IFN- $\gamma$ -*PmaCI* and pIBV-Vec-IFN- $\gamma$ -*SnaBI*, with the TAS-chIFN- $\gamma$  gene cassette in the correct orientation, and pIBV-Vec- $\gamma$ -NFIP*PmaCI* and pIBV-Vec- $\gamma$ -NFIS*SnaBI*, with the TAS-chIFN- $\gamma$  gene cassette in the opposite (incorrect) orientation, were identified for generating D-RNAs (Fig. 1).

**In vitro rescue of chIFN- $\gamma$ -containing D-RNAs.** In vitro T7-derived transcripts of D-RNAs IBV-Vec-IFN- $\gamma$ -*PmaCI*, IBV-Vec-IFN- $\gamma$ -*SnaBI*, IBV-Vec- $\gamma$ -NFIP*PmaCI*, and IBV-Vec- $\gamma$ -NFIS*SnaBI* were electroporated into IBV-infected CK cells, and progeny virus with D-RNAs was serially passaged on CK cells ( $P_0$  to  $P_6$ ). Northern blot analyses using the IBV 3'-UTR and chIFN- $\gamma$  probes on RNA isolated from  $P_3$  cells identified an RNA species of 6.8 kb (Fig. 2). This RNA was not present in cells infected with IBV only and corresponded in size to the in vitro T7-derived D-RNA transcript. The chIFN- $\gamma$ -specific probe did not hybridize to IBV gRNA or sg mRNAs, indicating that the 6.8-kb RNA represented D-RNAs containing the TAS-chIFN- $\gamma$  sequence. As expected, the chIFN- $\gamma$  probe detected D-RNAs IBV-Vec- $\gamma$ -NFIP*PmaCI* and IBV-Vec- $\gamma$ -NFIS*SnaBI*, with the TAS-chIFN- $\gamma$  sequence in the opposite orientation. The chIFN- $\gamma$  probe also detected two other RNAs of 1.7 kb (Fig. 2B, lane 3) and 5 kb (Fig. 2B, lane 4) following the rescue of D-RNAs IBV-Vec-IFN- $\gamma$ -*PmaCI* and IBV-Vec-IFN- $\gamma$ -*SnaBI*, respectively, in addition to the 6.8-kb D-RNA. These RNAs corresponded to the expected sizes of chIFN- $\gamma$  mRNAs expressed from the TAS-chIFN- $\gamma$  sequence in the D-RNAs. The IBV-Vec-IFN- $\gamma$ -*PmaCI* 1.7-kb chIFN- $\gamma$  mRNA was routinely observed in smaller amounts than the IBV-Vec-IFN- $\gamma$ -*SnaBI* 5-kb chIFN- $\gamma$  mRNA. The IBV 3'-UTR probe detected RNAs larger than the 6.8-kb D-RNA and the 7.3-kb IBV sg mRNA 2 (Fig. 2A) which were not detected by the chIFN- $\gamma$  probe (Fig. 2B). These RNAs were shown, by using Northern blot analysis and an IBV 5'-UTR probe (Fig. 3), to be new IBV-derived D-RNAs not containing the TAS-chIFN- $\gamma$  sequence.

To investigate the rescue profile of the D-RNAs, Northern blot analyses were carried out on RNA isolated from  $P_0$  to  $P_6$  CK cells containing D-RNAs IBV-Vec-IFN- $\gamma$ -*PmaCI* and IBV-Vec-IFN- $\gamma$ -*SnaBI* by using the IBV 5'-UTR, 3'-UTR, and chIFN- $\gamma$  probes (Fig. 3). The 6.8-kb D-RNAs were detected by the two IBV probes in RNA isolated from  $P_1$  to  $P_6$  CK cells (Fig. 3A, B, D, and E), and analyses using the chIFN- $\gamma$  probe confirmed that they contained the chIFN- $\gamma$  sequence (Fig. 3C and F). Both D-RNAs, irrespective of whether the chIFN- $\gamma$  sequence was inserted into the *PmaCI* or *SnaBI* site, were initially detected at  $P_1$  and increased in amount upon serial passage, with the largest amount in  $P_4$  CK cells, after which the amount of D-RNA decreased.

RNAs larger than the 6.8-kb chIFN- $\gamma$ -containing D-RNA and the IBV sg mRNA 2 were detected from  $P_3$  to  $P_6$  by using both IBV probes. The use of the IBV 5' probe indicated that the RNAs corresponded to new IBV-derived D-RNAs (Fig. 3A, B, D, and E). The new D-RNAs did not contain the chIFN- $\gamma$  sequence (Fig. 3C and F), indicating that they were derived from IBV gRNA, and were observed in increasing amounts in RNA isolated from  $P_3$  to  $P_6$  cells, with concomitant gradual loss of the 6.8-kb chIFN- $\gamma$ -containing D-RNAs (Fig. 3).

Analysis of  $P_3$ -derived RNA following the rescue of D-RNA

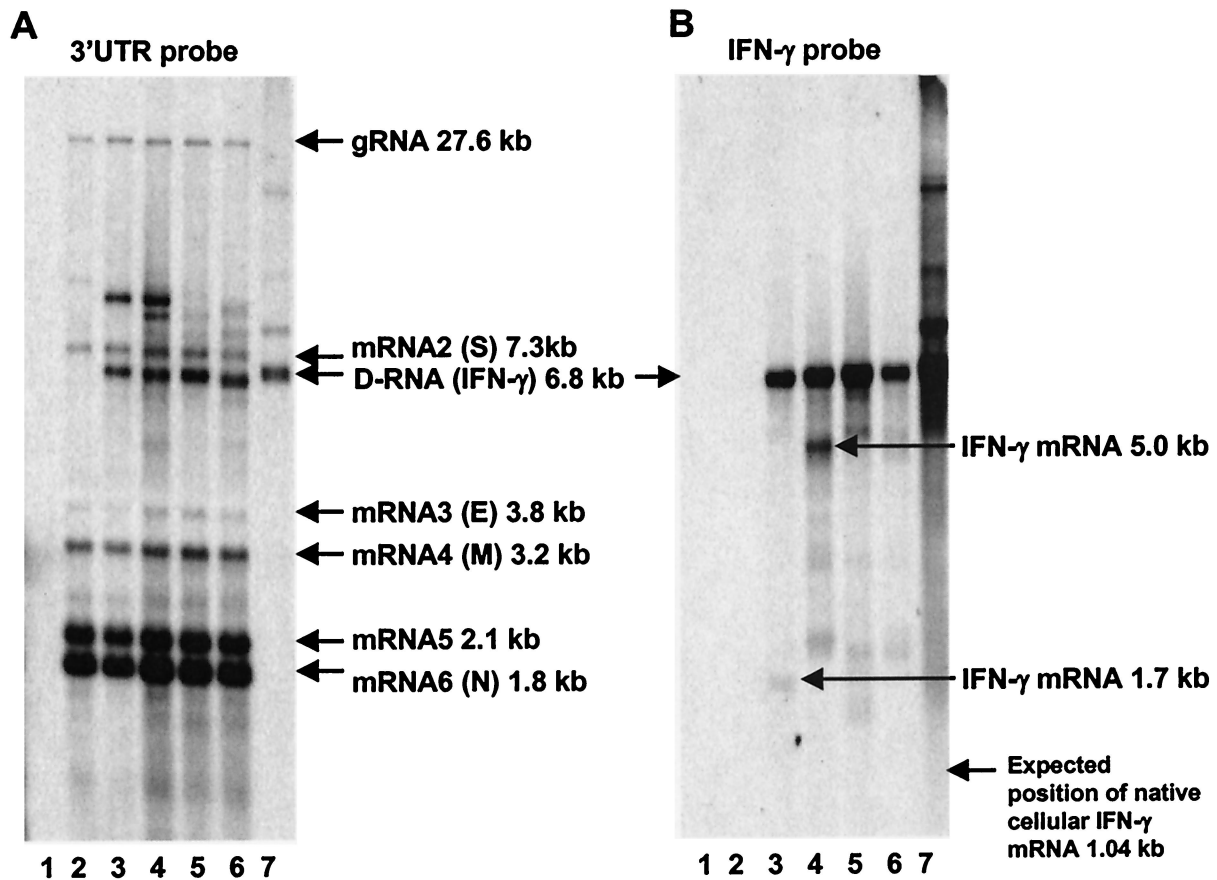


FIG. 2. Northern blot analysis of IBV-specific RNAs following rescue of chIFN- $\gamma$ -containing D-RNAs. Following electroporation of IBV-infected CK cells with in vitro T7-derived D-RNAs, progeny virus and D-RNAs were serially passaged ( $P_0$  to  $P_6$ ) on CK cells and total cytoplasmic RNA was extracted. RNA from  $P_3$  cells was electrophoresed in denaturing formaldehyde-agarose gels and subjected to Northern blotting, and IBV-derived RNAs were detected by using the 309-bp IBV 3'-UTR probe (A) and the 360-bp chIFN- $\gamma$  probe (B). The  $P_3$ -derived RNA samples analyzed were isolated from uninfected cells (lane 1); IBV-infected cells (lane 2); cells containing D-RNAs IBV-Vec-IFN- $\gamma$ *PmaCI*, IBV-Vec-IFN- $\gamma$ *SnaBI*, IBV-Vec- $\gamma$ -NFIP*maCI*, and IBV-Vec- $\gamma$ -NFI*SnaBI* (lanes 3 to 6, respectively); and in vitro T7-derived IBV-Vec-IFN- $\gamma$ *PmaCI* transcripts (lane 7). Arrows indicate IBV gRNA, sg mRNAs 2 to 6, TAS-chIFN- $\gamma$ -containing D-RNAs, and D-RNA-derived chIFN- $\gamma$  mRNAs. The RNAs detected between sg mRNAs 4 and 5 are observed routinely for all strains of IBV, as originally identified by Stern and Kennedy (38), and are of unknown origin. The RNAs migrating slower than IBV sg mRNA 2 were later shown to be new IBV-derived D-RNAs. The expected position of the full-length native cellular mRNA for chIFN- $\gamma$  (1,040 nt) is indicated on panel B. S, spike glycoprotein; E, small membrane protein; M, integral membrane protein; N, nucleocapsid protein.

IBV-Vec-IFN- $\gamma$ *SnaBI* identified a 5-kb D-RNA-derived chIFN- $\gamma$  mRNA. This mRNA was detected in RNA from  $P_1$  to  $P_6$  CK cells containing IBV-Vec-IFN- $\gamma$ *SnaBI*, with the amounts detected varying in accordance with the amounts of D-RNA present, the largest amount being detected at  $P_4$  (Fig. 3F). An RNA corresponding to the IBV-Vec-IFN- $\gamma$ *PmaCI* 1.7-kb chIFN- $\gamma$  mRNA was not detected following serial passage of the D-RNA (Fig. 3C). However, from the amounts of the RNA detected, the most likely explanation for this result was that the amount of the 1.7-kb chIFN- $\gamma$  mRNA was below the detection level of the analysis.

The Northern blot analyses showed that the two chIFN- $\gamma$ -containing D-RNAs with the TAS-chIFN- $\gamma$  insert in the correct orientation were rescued in IBV-infected CK cells upon serial passage. The analyses showed that D-RNA-derived chIFN- $\gamma$  mRNAs were transcribed, irrespective of the position of the TAS-chIFN- $\gamma$  insert, from the D-RNAs.

**Analysis of chIFN- $\gamma$  expression from D-RNAs.** The Northern blot analyses showed that D-RNAs containing the TAS-chIFN- $\gamma$  sequences in the correct orientation were rescued upon serial passage, but the analyses could not show whether biologically active chIFN- $\gamma$  was expressed. The biological assay for IFN- $\gamma$  is based on the fact that macrophages stimulated with IFN- $\gamma$  produce NO, along with other reactive nitrogen species, as one of several mechanisms to destroy intracellular pathogens. The chIFN- $\gamma$  bioassay involves stimulation of HD11 cells, a chicken macrophage cell line (3), with chIFN- $\gamma$  for the induction of NO, which accumulates as stable and quantifiable NO $_2^-$  in the HD11 culture medium.

Cell medium from the  $P_0$  to  $P_6$  CK cells, previously shown to contain the D-RNAs containing chIFN- $\gamma$ , was assayed for chIFN- $\gamma$  activity. Medium from cells containing D-RNAs IBV-Vec-IFN- $\gamma$ *PmaCI* and IBV-Vec-IFN- $\gamma$ *SnaBI* induced significantly larger amounts of NO, following stimulation of HD11

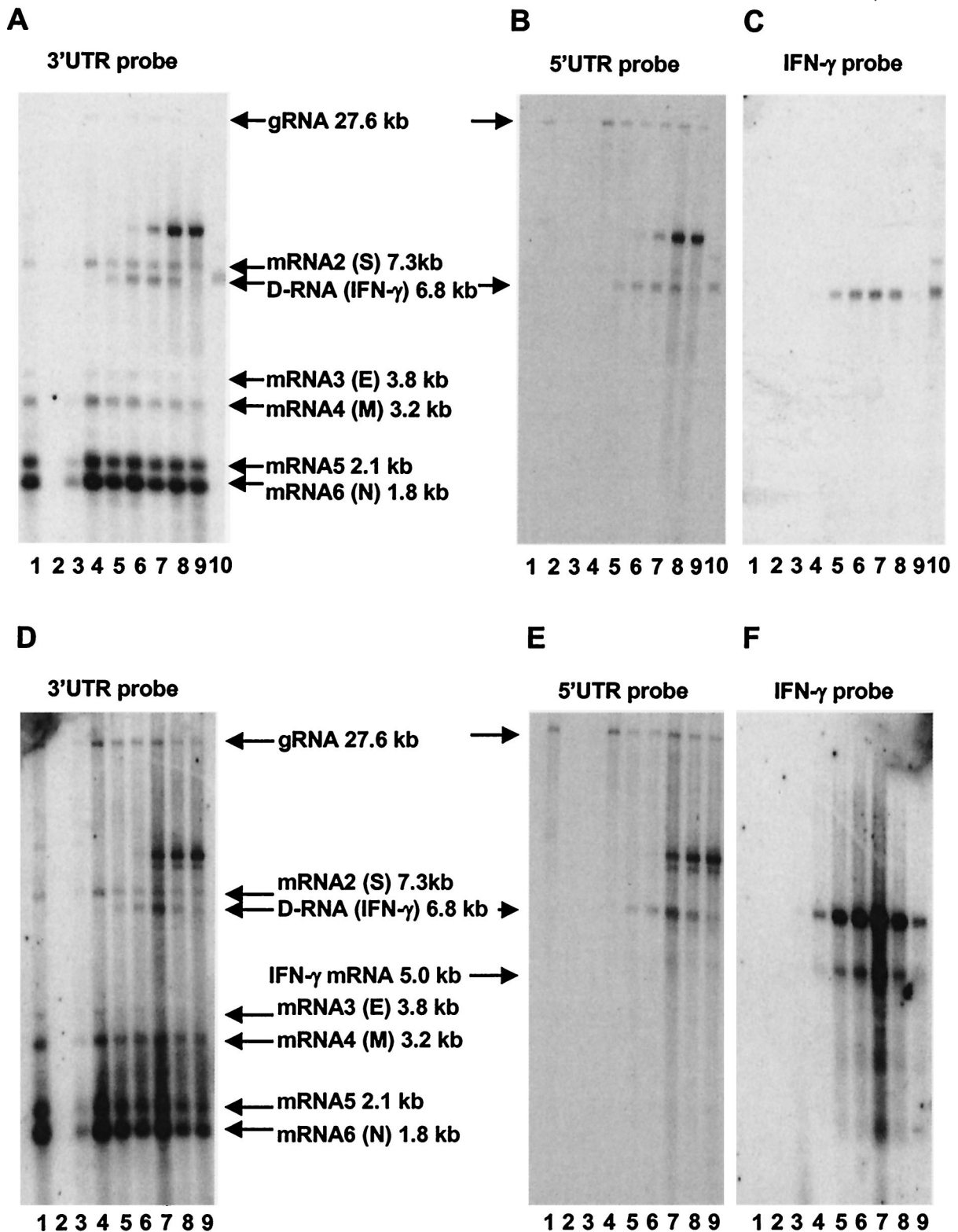


FIG. 3. Northern blot analysis of IBV-specific RNAs following serial passage of D-RNAs IBV-Vec-IFN- $\gamma$ PmaCI and IBV-Vec-IFN- $\gamma$ SnaBI. RNAs isolated from P<sub>0</sub> to P<sub>6</sub> CK cells were analyzed for the presence of D-RNAs IBV-Vec-IFN- $\gamma$ PmaCI (A to C) and IBV-Vec-IFN- $\gamma$ SnaBI (D to F). IBV-derived RNAs were detected by using the 309-bp IBV 3'-UTR probe (A and D), the 209-bp IBV 5'-UTR probe (B and E), and the 360-bp chIFN- $\gamma$  probe (C and F). The RNA samples analyzed were isolated from IBV-infected cells (lane 1), uninfected cells (lane 2), and P<sub>0</sub> to P<sub>6</sub> cells containing D-RNAs IBV-Vec-IFN- $\gamma$ PmaCI (A to C, lanes 3 to 9) and IBV-Vec-IFN- $\gamma$ SnaBI (D to F, lanes 3 to 9). (A to C) Lanes 10 correspond to in vitro T7-derived IBV-Vec-IFN- $\gamma$ PmaCI. Arrows indicate IBV gRNA, sg mRNAs, and TAS-chIFN- $\gamma$ -containing D-RNAs. The RNAs migrating slower than IBV sg mRNA 2, detected in RNA samples isolated from P<sub>3</sub> to P<sub>6</sub> cells (A, B, D, and E, lanes 6), are new IBV-derived D-RNAs. Analysis of RNA following passage of IBV-Vec-IFN- $\gamma$ SnaBI identified the D-RNA-derived chIFN- $\gamma$  mRNA (F, lanes 5 to 8). S, spike glycoprotein; E, small membrane protein; M, integral membrane protein; N, nucleocapsid protein.

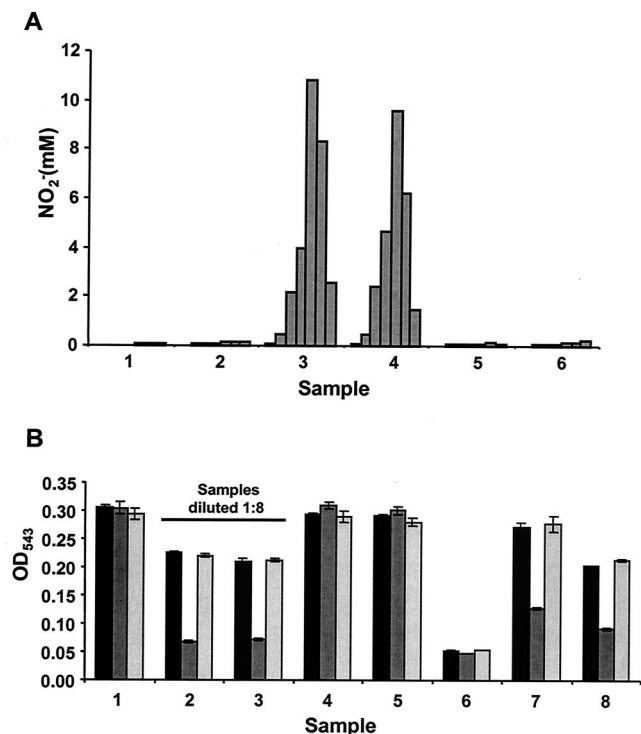


FIG. 4. Analysis of IFN activity in cell medium following in vitro passage of  $\text{chIFN-}\gamma$ -containing D-RNAs. (A) NO detected from HD11 cells, following stimulation with cell medium samples from uninfected cells (sample 1); IBV-infected cells (six passages) (sample 2); and  $P_0$  to  $P_6$  cells containing D-RNAs IBV-Vec-IFN- $\gamma$ *Pma*CI, IBV-Vec-IFN- $\gamma$ *Sna*BI, IBV-Vec- $\gamma$ -NFIP*ma*CI, and IBV-Vec- $\gamma$ -NFIS*na*BI (samples 3 to 6, respectively). (B)  $\text{chIFN-}\gamma$ -neutralizing bioassays using anti- $\text{chIFN-}\gamma$  MAb 1E-12. Cell medium samples were preincubated for 2 h with medium alone (black bars), MAb 1E-12 (dark grey bars), or the isotype control Ab CC305 (light grey bars). Antibodies were diluted 1:1,000 for the assay. Ab-treated samples, analyzed for their ability to induce NO from HD11 cells, were from IBV-infected cells (sample 1), cells containing D-RNAs IBV-Vec-IFN- $\gamma$ *Pma*CI and IBV-Vec-IFN- $\gamma$ *Sna*BI (used at 1:8 dilutions) (samples 2 and 3, respectively), cells containing D-RNAs IBV-Vec- $\gamma$ -NFIP*ma*CI and IBV-Vec- $\gamma$ -NFIS*na*BI (samples 4 and 5, respectively), medium alone (sample 6), and recombinant  $\text{chIFN-}\gamma$  at 1:125 and 1:250 dilutions (samples 7 and 8, respectively). Nitrite resulting from the induced NO in the HD11 cell medium samples was quantified by using a variation of the Griess assay, measuring absorbance at 543 nm. The histograms represent the midpoints taken from the linear portions of titration curves calculated from the means of results for triplicates of each sample (A) and the means of results for triplicate samples ( $\pm$  standard errors) (B). OD<sub>543</sub>, optical density at 543 nm.

cells, than any of the controls (Fig. 4A). In contrast, medium from cells containing D-RNAs IBV-Vec- $\gamma$ -NFIP*ma*CI and IBV-Vec- $\gamma$ -NFIS*na*BI did not induce larger amounts of NO than the controls. Controls involved medium from uninfected CK and IBV-infected CK cells. The amounts of NO induced by using medium from control samples and from cells containing D-RNAs with the TAS- $\text{chIFN-}\gamma$  insert in the incorrect orientation were similar and likely to result from the presence of IFN- $\alpha$  or IFN- $\beta$ . The IFN- $\gamma$  bioassay also detects IFN- $\alpha$  and IFN- $\beta$ , previously shown to be produced by IBV-infected cells (16, 28, 29).

To confirm that the NO detected by the IFN- $\gamma$  bioassay was

due to the induction of HD11 cells by IFN- $\gamma$ , and not by IFN- $\alpha$  and IFN- $\beta$ , which also stimulate the production of NO, a neutralizing bioassay was carried out. Samples of cell medium were preincubated with the  $\text{chIFN-}\gamma$ -neutralizing MAb 1E-12 and analyzed with the IFN- $\gamma$  bioassay. Samples were preincubated with medium and Ab CC305, an isotype control Ab against bovine granulocyte-macrophage colony-stimulating factor. For comparative purposes, recombinant  $\text{chIFN-}\gamma$  was included as a positive control sample. NO induction, using medium from cells containing D-RNAs IBV-Vec-IFN- $\gamma$ *Pma*CI and IBV-Vec-IFN- $\gamma$ *Sna*BI, with the TAS- $\text{chIFN-}\gamma$  sequence in the correct orientation, was reduced following preincubation of the samples with the neutralizing MAb 1E-12 (Fig. 4B). The amount of neutralizing MAb 1E-12 used was sufficient to neutralize all the  $\text{chIFN-}\gamma$  in the solution. To confirm this, the neutralizing activity of the MAb had been titrated before use in this experiment. Levels of remaining activity were assumed to be due to IFN- $\alpha$  and IFN- $\beta$ . These levels were consistent with those seen in a previous study using this neutralizing MAb (19). A similar reduction in NO induction was observed when the recombinant  $\text{chIFN-}\gamma$  was preincubated with the MAb 1E-12. In contrast, the NO induced by using medium from cells containing D-RNAs IBV-Vec- $\gamma$ -NFIP*ma*CI and IBV-Vec- $\gamma$ -NFIS*na*BI, with the TAS- $\text{chIFN-}\gamma$  sequence in the incorrect orientation, was not affected by the addition of the neutralizing MAb 1E-12. This indicated that the NO detected resulted from induction with chicken IFN- $\alpha$  or IFN- $\beta$  rather than  $\text{chIFN-}\gamma$  in the cell medium (Fig. 4B). These results showed that the NO induction observed by using samples taken from cells containing D-RNAs IBV-Vec-IFN- $\gamma$ *Pma*CI and IBV-Vec-IFN- $\gamma$ *Sna*BI resulted from the presence of  $\text{chIFN-}\gamma$  in the cell medium and confirmed that the D-RNAs expressed biologically active  $\text{chIFN-}\gamma$ .

Induction of NO, using medium from cells containing D-RNAs IBV-Vec-IFN- $\gamma$ *Pma*CI and IBV-Vec-IFN- $\gamma$ *Sna*BI, was observed from  $P_0$  and increased to  $P_4$ , followed by a decrease in NO at  $P_5$  to  $P_6$ . This indicated that the amounts of  $\text{chIFN-}\gamma$  expressed increased upon serial passage of the D-RNAs, with a peak of activity in  $P_4$  CK cells followed by a decrease in activity (Fig. 4A). This result correlated with the Northern blot analyses in which the amounts of the D-RNAs and one of the D-RNA-derived  $\text{chIFN-}\gamma$  mRNAs followed the same pattern over serial passage. Results of the bioassay also showed that there were no significant differences in the amounts of NO induced whether the samples came from cells containing TAS- $\text{chIFN-}\gamma$  inserted into the *Pma*CI or from cells containing TAS- $\text{chIFN-}\gamma$  inserted into the *Sna*BI site of CD-61 (Fig. 4A), indicating that both D-RNAs expressed similar amounts of  $\text{chIFN-}\gamma$ .

**In ovo rescue of  $\text{chIFN-}\gamma$ -containing D-RNAs.** Previous work to determine whether IBV D-RNAs could be passaged in vivo by using embryonated eggs (in ovo) had required subsequent passage of a D-RNA expressing chloramphenicol acetyltransferase (CAT) on indicator CK cells. Subsequent analysis of cell lysates demonstrated the presence of CAT (5, 11). A limitation of these experiments was that replication may not have occurred in ovo and that rescue on the CK cells could have resulted from virus and D-RNA present in the allantoic fluid from the initial inoculum, although rescue following dilution in the allantoic fluid would be indicative of replication in

ovo. The secretion of chIFN- $\gamma$  into cell medium following expression from the D-RNAs described in this work provided a means of determining whether IBV D-RNAs can be replicated in ovo.

Following serial passage of D-RNAs IBV-Vec-IFN- $\gamma$ *PmaCI* and IBV-Vec-IFN- $\gamma$ *SnaBI*, the largest amounts of D-RNA detected with concomitant expression of chIFN- $\gamma$  occurred in P<sub>4</sub> cells (Fig. 3 and 4). Consequently, we decided to use progeny virus (V<sub>4</sub>) containing the D-RNAs from P<sub>3</sub> cells to determine whether the D-RNAs could be rescued in ovo. Virus (V<sub>4</sub>) from P<sub>3</sub> cells, representing virus that was one passage away from peak chIFN- $\gamma$  activity, was used to infect 10-day-old specific-pathogen-free embryonated eggs. At 16 h postinoculation, allantoic fluid was clarified and used to infect CK cells to confirm that the D-RNAs could be passed from embryonated eggs. The fluid was also used for chIFN- $\gamma$  bioassays to analyze for the presence of any chIFN- $\gamma$  resulting from the replication of the D-RNAs in ovo.

IFN- $\gamma$  bioassays showed that allantoic fluid and CK cell medium samples, following passage of D-RNAs IBV-Vec-IFN- $\gamma$ *PmaCI* and IBV-Vec-IFN- $\gamma$ *SnaBI*, contained amounts of chIFN- $\gamma$  that were up to 64-fold and 10-fold larger, respectively, as measured by NO levels, than those of the controls (Fig. 5A), indicating that the D-RNAs had replicated in ovo. The amounts of NO induced following infection with IBV only and passage of D-RNAs containing the TAS-chIFN- $\gamma$  gene construct in the antisense orientation were all similar, with NO induction presumably due to the presence of IFN- $\alpha$  or IFN- $\beta$ . The amounts of chIFN- $\gamma$ , as measured by NO levels, in allantoic fluid following in ovo passage of D-RNAs IBV-Vec-IFN- $\gamma$ *PmaCI* and IBV-Vec-IFN- $\gamma$ *SnaBI* were larger than those found in CK cell medium following subsequent in vitro passage of the D-RNAs. This result was anticipated, as the in ovo passage was equivalent to P<sub>4</sub> and CK passage was equivalent to P<sub>5</sub> when equated with in vitro passage of the D-RNAs.

A neutralizing IFN- $\gamma$  bioassay was again performed to confirm that the NO induced resulted from IFN- $\gamma$  and not from IFN- $\alpha$  and IFN- $\beta$ . Allantoic fluid and CK cell medium samples were preincubated with MAb 1E-12, medium, and the isotype control Ab CC305 for 2 h prior to the IFN- $\gamma$  bioassay (Fig. 5B). The amounts of NO induced by using samples from embryonated eggs (Fig. 5B, samples 1 and 2) and CK cells (Fig. 5B, samples 9 and 10) infected with IBV containing D-RNAs IBV-Vec-IFN- $\gamma$ *PmaCI* and IBV-Vec-IFN- $\gamma$ *SnaBI* were similar for both D-RNAs both in ovo and in vitro and were similarly reduced following preincubation with MAb 1E-12. A similar reduction in NO induction was observed following preincubation of recombinant chIFN- $\gamma$  with MAb 1E-12 (Fig. 5B, sample 7), indicating that the IFN activities detected in the allantoic fluid and CK cell medium samples resulted from IFN- $\gamma$ . In contrast, the amounts of NO induced by using samples from embryonated eggs and CK cells infected with IBV containing D-RNAs IBV-Vec- $\gamma$ -NFIP*PmaCI* and IBV-Vec- $\gamma$ -NFIS*SnaBI* and from IBV infection alone were not reduced following preincubation with MAb 1E-12 (Fig. 5B). This indicated that the IFN activities observed following in ovo passage of these D-RNAs and IBV alone resulted from the induction of IFN- $\alpha$  and IFN- $\beta$  and not from IFN- $\gamma$ .

These results confirmed that D-RNAs IBV-Vec-IFN- $\gamma$ *PmaCI* and IBV-Vec-IFN- $\gamma$ *SnaBI* expressed biologically ac-

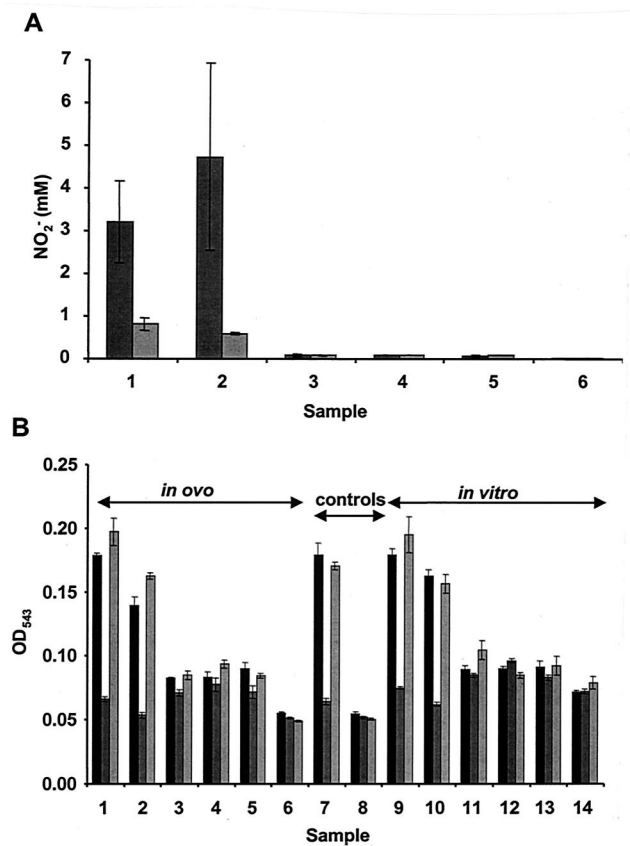


FIG. 5. Analysis of IFN activity in allantoic fluid following in ovo passage of chIFN- $\gamma$ -containing D-RNAs. The chIFN- $\gamma$ -containing D-RNAs were initially passed in embryonated eggs, and progeny virus containing the D-RNAs in the allantoic fluid was passaged on indicator CK cells. (A) NO detected from HD11 cells following stimulation with allantoic fluid (dark grey bars) or CK cell medium (light grey bars) from passage of D-RNAs IBV-Vec-IFN- $\gamma$ *PmaCI*, IBV-Vec-IFN- $\gamma$ *SnaBI*, IBV-Vec- $\gamma$ -NFIP*PmaCI*, and IBV-Vec- $\gamma$ -NFIS*SnaBI* (samples 1 to 4, respectively); IBV-infected cells (sample 5); and uninfected cells (sample 6). The histogram represents the midpoints taken from the linear portions of titration curves calculated from the means ( $\pm$  standard errors) of results for triplicates of each sample. (B) chIFN- $\gamma$ -neutralizing bioassays in which samples, preincubated for 2 h with medium alone (black bars), MAb 1E-12 (dark grey bars), or CC305 (light grey bars), were analyzed for their ability to induce NO from HD11 cells consisted of allantoic fluid (samples 1 to 6); CK cell media (samples 9 to 14); recombinant chIFN- $\gamma$  diluted 1:2,000 (sample 7); and media alone (sample 8). Samples 1 to 4 and 9 to 12 were from allantoic fluid and CK cell medium, respectively, following passage of D-RNAs IBV-Vec-IFN- $\gamma$ *PmaCI* (diluted 1:8), IBV-Vec-IFN- $\gamma$ *SnaBI* (diluted 1:8), IBV-Vec- $\gamma$ -NFIP*PmaCI*, and IBV-Vec- $\gamma$ -NFIS*SnaBI*, respectively. Samples 5 to 6 and 13 to 14 were from allantoic fluid and CK cell medium, respectively, from cells infected with IBV (5 and 13) or uninfected cells (6 and 14). Antibodies were diluted 1:1,000 for the assay. The histogram represents the means ( $\pm$  standard errors) of results for triplicate samples. OD<sub>543</sub>, optical density at 543 nm.

tive chIFN- $\gamma$  following helper virus-dependent replication in ovo.

## DISCUSSION

The construction of a series of IBV-based D-RNAs containing the chIFN- $\gamma$  sequence under the control of an IBV TAS

has been described. We have shown that IBV D-RNAs containing the chIFN- $\gamma$  gene were incorporated into virus particles and expressed biologically active chIFN- $\gamma$  in vitro and in vivo.

Serial passage of the chIFN- $\gamma$ -containing D-RNAs followed the same pattern of both D-RNA replication and heterologous protein expression that we have previously observed for the expression of the heterologous reporter genes encoding CAT (39) and luciferase (13) from IBV-based D-RNAs. Both detection of the D-RNA and expression of chIFN- $\gamma$  increased from P<sub>0</sub> to P<sub>4</sub> and decreased thereafter. No differences in the amounts of D-RNA detected or in chIFN- $\gamma$  activities were observed whether the TAS-chIFN- $\gamma$  cassette was inserted in domain I (IBV-Vec-IFN- $\gamma$ SnaBI), interrupting the D-RNA-specific ORF, or domain III (IBV-Vec-IFN- $\gamma$ PmaCI), not interrupting the D-RNA-specific ORF, of D-RNA CD-61.

A D-RNA-derived chIFN- $\gamma$  mRNA synthesized from IBV-Vec-IFN- $\gamma$ SnaBI was detectable upon serial passage of the D-RNA (Fig. 2B and 3F). Although a D-RNA-derived chIFN- $\gamma$  mRNA synthesized from IBV-Vec-IFN- $\gamma$ PmaCI was initially detected (Fig. 2B), it was synthesized in smaller amounts, in relation to the D-RNA, than the mRNA from IBV-Vec-IFN- $\gamma$ SnaBI. The observed levels of subgenomic RNAs (sgRNAs) transcribed, under the control of the gene 5 TAS, from CD-61-derived D-RNAs were far less than the amounts observed for the transcription of sg mRNA 5 from genomic RNA. Similar observations have been made following transcription of sgRNAs from other coronavirus-derived D-RNAs. The altered transcription levels may be connected to the observation that D-RNAs may replicate in a manner analogous to the transcription of sg mRNAs from genomic RNA (40), thereby affecting the levels of transcription of D-RNA-derived sgRNAs, or the levels may result from the altered context of the TAS within the D-RNA. The sequences flanking the TASs of heterologous genes in transmissible gastroenteritis virus-derived D-RNAs have been shown to alter the transcription of D-RNA-derived sgRNAs (1). The amounts of chIFN- $\gamma$  secreted from cells containing the D-RNAs were similar, as observed from the induction of NO from HD11 cells, indicating that the D-RNAs expressed similar amounts of active chIFN- $\gamma$ . Similar results were observed for the expression of  $\beta$ -glucuronidase (GUS) from a transmissible gastroenteritis virus-based D-RNA, in which the D-RNA-derived GUS mRNA was transcribed in smaller amounts in P<sub>2</sub> cells than in P<sub>5</sub> cells, although the amounts of GUS protein expressed were the same (2).

Although its main role is in driving a Th1 cell-mediated response against intracellular pathogens, including viruses, IFN- $\gamma$  can have a direct antiviral effect. Like IFN- $\alpha$  and IFN- $\beta$ , but to a much lesser extent, it can induce oligoadenylate synthetase and RNA-dependent protein kinase PKR, both important components of IFN-induced antiviral responses (8, 14, 34). It was therefore possible that expression of chIFN- $\gamma$  from the D-RNAs might interfere with replication of the helper virus. A murine IFN- $\gamma$ -containing D-RNA of the murine coronavirus mouse hepatitis virus (MHV) expressed murine IFN- $\gamma$  that resulted in a slight reduction in virus titer (0.5 log<sub>10</sub>) at low multiplicities of infection, suggesting that the murine IFN- $\gamma$  had a weak antiviral activity (42). In contrast, we observed no significant differences in virus titers resulting from expression of the chIFN- $\gamma$  from any of the IBV D-RNAs (data not

shown), suggesting that the chIFN- $\gamma$  did not have an appreciable antiviral effect on the helper IBV.

The murine IFN- $\gamma$ -containing MHV D-RNA was not detected beyond P<sub>4</sub> (42), whereas the IBV-based chIFN- $\gamma$ -containing D-RNAs were rescued for at least six passages. This observation reflects our previous studies on the expression of heterologous genes from IBV-CD-61-based D-RNAs. Expression of heterologous genes or coronavirus-derived genes from other coronavirus D-RNAs also resulted in loss of the D-RNAs. For example, expression of CAT and hemagglutinin esterase from MHV D-RNAs was not detected beyond P<sub>2</sub> (20) and P<sub>3</sub> (43), respectively. The most likely explanation for the instability of coronavirus D-RNAs expressing heterologous genes is intolerance of the heterologous sequence within the D-RNA. D-RNAs evolve by the removal of unnecessary sequences. Therefore, the presence of a heterologous sequence may impart some innate instability into the RNA or affect replication and/or packaging of the D-RNA; i.e., D-RNAs containing heterologous or nonrequired sequences are less fitted for replication than D-RNAs with minimal required sequences. We detected additional RNA species, which were larger than the chIFN- $\gamma$ -containing D-RNAs and IBV sg mRNA 2, from P<sub>3</sub> which increased in amount upon serial passage. The new RNAs were not detected by the chIFN- $\gamma$ -specific probe but by the IBV 5' probe, showing that they contained sequences derived from the 5' end of the IBV genome and were therefore new D-RNAs. As determined from their sizes, the new D-RNAs were not from the loss of the chIFN- $\gamma$  sequence. An explanation for the loss of the chIFN- $\gamma$ -containing D-RNAs beyond P<sub>4</sub> was the generation of more stable D-RNAs from P<sub>3</sub> that eventually resulted, due to competition, in the loss of the chIFN- $\gamma$ -containing D-RNAs.

Overall, we have demonstrated that in vitro passage of the chIFN- $\gamma$ -containing D-RNAs resulted in expression of biologically active chIFN- $\gamma$  secreted into cell culture medium. This observation allowed us to demonstrate that IBV D-RNAs can be replicated in ovo from the presence of biologically active chIFN- $\gamma$  secreted into the allantoic fluid and subsequent passage on indicator CK cells.

#### ACKNOWLEDGMENTS

Karen Hackney held a Research Studentship from the British Egg Marketing Board Research and Education Trust. This work was supported by the Biotechnology and Biological Sciences Research Council (BBSRC) and the Department of Environment, Food and Rural Affairs (DEFRA) project code OD0712.

#### REFERENCES

- Alonso, S., A. Izeta, I. Sola, and L. Enjuanes. 2002. Transcription regulatory sequences and mRNA expression levels in the coronavirus transmissible gastroenteritis virus. *J. Virol.* **76**:1293–1308.
- Alonso, S., I. Sola, J. P. Teifke, I. Reimann, A. Izeta, M. Balasch, J. Planaduran, R. J. Moormann, and L. Enjuanes. 2002. *In vitro* and *in vivo* expression of foreign genes by transmissible gastroenteritis coronavirus-derived minigenomes. *J. Gen. Virol.* **83**:567–579.
- Beug, H., A. von Kirchbach, G. Doderlein, J. F. Conscience, and T. Graf. 1979. Chicken hematopoietic cells transformed by seven strains of defective avian leukemia viruses display three distinct phenotypes of differentiation. *Cell* **18**:375–390.
- Bournsnel, M. E., T. D. Brown, I. J. Foulds, P. F. Green, F. M. Tomley, and M. M. Binns. 1987. Completion of the sequence of the genome of the coronavirus avian infectious bronchitis virus. *J. Gen. Virol.* **68**:57–77.
- Britton, P., K. Stirrups, K. Dalton, K. Shaw, S. Evans, B. Neuman, B. Dove, R. Casais, and D. Cavanagh. 2001. Use of an infectious bronchitis virus D-RNA as an RNA vector. *Adv. Exp. Med. Biol.* **494**:507–512.



6. Cavanagh, D., K. Mawditt, M. Sharma, S. E. Drury, H. L. Ainsworth, P. Britton, and R. E. Gough. 2001. Detection of a coronavirus from turkey poult in Europe genetically related to infectious bronchitis virus of chickens. *Avian Pathol.* **30**:365–378.
7. Cavanagh, D., K. Mawditt, D. D. B. Welchman, P. Britton, and R. E. Gough. 2002. Coronaviruses from pheasants (*Phasianus colchicus*) are genetically closely related to coronaviruses of domestic fowl (infectious bronchitis virus) and turkeys. *Avian Pathol.* **31**:81–93.
8. De Maeyer, E., and J. De Maeyer-Guinard. 1998. Interferons, p. 491–516. In A. Thomson (ed.), *The cytokine handbook*, 3rd ed. Academic Press, San Diego, Calif.
9. Dhinakar-Raj, G., and R. C. Jones. 1997. Infectious bronchitis virus: immunopathogenesis of infection in the chicken. *Avian Pathol.* **26**:677–706.
10. Digby, M. R., and J. W. Lowenthal. 1995. Cloning and expression of the chicken interferon- $\gamma$  gene. *J. Interferon Cytokine Res.* **15**:939–945.
11. Dove, B. 2002. Ph.D. thesis. University of Reading, Reading, United Kingdom.
12. Enjuanes, L., W. J. Spaan, E. J. Snijder, and D. Cavanagh. 2000. Nidovirales, p. 827–834. In M. H. V. van Regenmortel, C. M. Fauquet, D. H. L. Bishop, E. B. Carsten, M. K. Estes, S. M. Lemon, D. J. McGeoch, J. Maniloff, M. A. Mayo, C. R. Pringle, and R. B. Wickner (ed.), *Virus taxonomy: classification and nomenclature of viruses*. Academic Press, New York, N.Y.
13. Evans, S., D. Cavanagh, and P. Britton. 2000. Utilizing fowlpox virus recombinants to generate defective RNAs of the coronavirus infectious bronchitis virus. *J. Gen. Virol.* **81**:2855–2865.
14. Goodbourn, S., L. Didcock, and R. E. Randall. 2000. Interferons: cell signalling, immune modulation, antiviral response and virus countermeasures. *J. Gen. Virol.* **81**:2341–2364.
15. Hiscox, J. A., K. L. Mawditt, D. Cavanagh, and P. Britton. 1995. Investigation of the control of coronavirus subgenomic mRNA transcription by using T7-generated negative-sense RNA transcripts. *J. Virol.* **69**:6219–6227.
16. Holmes, H. C., and J. H. Darbyshire. 1978. Induction of chicken interferon by avian infectious bronchitis virus. *Res. Vet. Sci.* **25**:178–181.
17. Izeta, A., C. Smerdou, S. Alonso, Z. Penzes, A. Mendez, J. Plana-Duran, and L. Enjuanes. 1999. Replication and packaging of transmissible gastroenteritis coronavirus-derived synthetic minigenomes. *J. Virol.* **73**:1535–1545.
18. Lambrecht, B., M. Gonze, G. Meulemans, and T. P. van den Berg. 2000. Production of antibodies against chicken interferon- $\gamma$ : demonstration of neutralizing activity and development of a quantitative ELISA. *Vet. Immunol. Immunopathol.* **74**:137–144.
19. Lawson, S., L. Rothwell, B. Lambrecht, K. Howes, K. Venugopal, and P. Kaiser. 2001. Turkey and chicken interferon- $\gamma$ , which share high sequence identity, are biologically cross-reactive. *Dev. Comp. Immunol.* **25**:69–82.
20. Liao, C. L., X. Zhang, and M. M. Lai. 1995. Coronavirus defective-interfering RNA as an expression vector: the generation of a pseudorecombinant mouse hepatitis virus expressing hemagglutinin-esterase. *Virology* **208**:319–327.
21. Lillehoj, H. S., and K. D. Choi. 1998. Recombinant chicken interferon- $\gamma$  mediated inhibition of *Eimeria tenella* development in vitro and reduction of oocyst production and body weight loss following *Eimeria acervulina* challenge infection. *Avian Dis.* **42**:307–314.
22. Lin, Y. J., and M. M. Lai. 1993. Deletion mapping of a mouse hepatitis virus defective interfering RNA reveals the requirement of an internal and discontinuous sequence for replication. *J. Virol.* **67**:6110–6118.
23. Lowenthal, J. W., T. E. O'Neil, M. Broadway, A. D. Strom, M. R. Digby, M. Andrew, and J. J. York. 1998. Coadministration of IFN- $\gamma$  enhances antibody responses in chickens. *J. Interferon Cytokine Res.* **18**:617–622.
24. Lowenthal, J. W., J. J. York, T. E. O'Neil, R. A. Steven, D. G. Strom, and M. R. Digby. 1998. Potential use of cytokine therapy in poultry. *Vet. Immunol. Immunopathol.* **63**:191–198.
25. Masters, P. S. 1999. Reverse genetics of the largest RNA viruses. *Adv. Virus Res.* **53**:245–264.
26. McCormick, A. L., M. S. Thomas, and A. W. Heath. 2001. Immunization with an interferon- $\gamma$ -gp120 fusion protein induces enhanced immune responses to human immunodeficiency virus gp120. *J. Infect. Dis.* **184**:1423–1430.
27. Min, W., H. S. Lillehoj, J. Burnside, K. C. Weining, P. Staeheli, and J. J. Zhu. 2001. Adjuvant effects of IL-1 $\beta$ , IL-2, IL-8, IL-15, IFN- $\alpha$ , IFN- $\gamma$ , TGF- $\beta$ 4 and lymphotactin on DNA vaccination against *Eimeria acervulina*. *Vaccine* **20**:267–274.
28. Otsuki, K., J. Maeda, H. Yamamoto, and M. Tsubokura. 1979. Studies on avian infectious bronchitis virus (IBV). III. Interferon induction by and sensitivity to interferon of IBV. *Arch. Virol.* **60**:249–255.
29. Otsuki, K., T. Nakamura, Y. Kawaoka, and M. Tsubokura. 1988. Interferon induction by several strains of avian infectious bronchitis virus, a coronavirus, in chickens. *Acta Virol.* **32**:55–59.
30. Penzes, Z., K. Tibbles, K. Shaw, P. Britton, T. D. Brown, and D. Cavanagh. 1994. Characterization of a replicating and packaged defective RNA of avian coronavirus infectious bronchitis virus. *Virology* **203**:286–293.
31. Penzes, Z., C. Wroe, T. D. Brown, P. Britton, and D. Cavanagh. 1996. Replication and packaging of coronavirus infectious bronchitis virus defective RNAs lacking a long open reading frame. *J. Virol.* **70**:8660–8668.
32. Rautenschlein, S., J. M. Sharma, B. J. Winslow, J. McMillen, D. Junker, and M. Cochran. 1999. Embryo vaccination of turkeys against Newcastle disease infection with recombinant fowlpox virus constructs containing interferons as adjuvants. *Vaccine* **18**:426–433.
33. Sambrook, J., E. F. Fritsch, and T. Maniatis. 1989. *Molecular cloning: a laboratory manual*, 2nd ed. Cold Spring Harbor Laboratory, Cold Spring Harbor, N.Y.
34. Samuel, C. E. 2001. Antiviral actions of interferons. *Clin. Microbiol. Rev.* **14**:778–809.
35. Sawicki, S. G., and D. L. Sawicki. 1990. Coronavirus transcription: subgenomic mouse hepatitis virus replicative intermediates function in RNA synthesis. *J. Virol.* **64**:1050–1056.
36. Sawicki, S. G., and D. L. Sawicki. 1998. A new model for coronavirus transcription. *Adv. Exp. Med. Biol.* **440**:215–219.
37. Schijns, V. E., N. C. Scholtes, H. I. Zuilekom, L. E. Sanders, L. Nicolson, and D. J. Argyle. 2002. Facilitation of antibody forming responses to viral vaccine antigens in young cats by recombinant baculovirus-expressed feline IFN- $\gamma$ . *Vaccine* **20**:1718–1724.
38. Stern, D. F., and S. I. T. Kennedy. 1980. Coronavirus multiplication strategy. I. Identification and characterisation of virus-specific RNA. *J. Virol.* **34**:665–674.
39. Stirrups, K., K. Shaw, S. Evans, K. Dalton, R. Casais, D. Cavanagh, and P. Britton. 2000. Expression of reporter genes from the defective RNA CD-61 of the coronavirus infectious bronchitis virus. *J. Gen. Virol.* **81**:1687–1698.
40. Stirrups, K., K. Shaw, S. Evans, K. Dalton, D. Cavanagh, and P. Britton. 2000. Leader switching occurs during the rescue of defective RNAs by heterologous strains of the coronavirus infectious bronchitis virus. *J. Gen. Virol.* **81**:791–801.
41. Yilma, T., S. Owens, E. H. Fennie, and K. P. Anderson. 1989. Enhancement of primary and secondary immune responses by interferon- $\gamma$ . *Adv. Exp. Med. Biol.* **251**:145–152.
42. Zhang, X., D. R. Hinton, D. J. Cua, S. A. Stohlman, and M. M. Lai. 1997. Expression of interferon- $\gamma$  by a coronavirus defective-interfering RNA vector and its effect on viral replication, spread, and pathogenicity. *Virology* **233**:327–338.
43. Zhang, X., D. R. Hinton, S. Park, B. Parra, C. L. Liao, M. M. Lai, and S. A. Stohlman. 1998. Expression of hemagglutinin/esterase by a mouse hepatitis virus coronavirus defective-interfering RNA alters viral pathogenesis. *Virology* **242**:170–183.